

Article

Immobilization Behavior and Mechanism of Cd²⁺ by Sulfate-Reducing Bacteria in Anoxic Environments

Lang Liao ¹, Qian Li ^{1,*}, Yongbin Yang ¹, Rui Xu ^{1,2} and Yan Zhang ¹

¹ School of Minerals Processing and Bioengineering, Central South University, Changsha 410083, China; 215611021@csu.edu.cn (L.L.)

² Faculty of Environmental Science and Engineering, Kunming University of Science and Technology, Kunming 650500, China

* Correspondence: csuliqian208018@csu.edu.cn

Abstract: It is vital to remove cadmium from wastewater because of its potential harm to the natural environment and human health. It was found that sulfate-reducing bacteria (SRB) had a good fixing effect on Cd under a strict anaerobic environment. However, there are few reports on the immobilization effect and mechanism of SRB on Cd in an anoxic environment. This study revealed the effects of initial Cd²⁺ concentration, initial SO₄²⁻ concentration, temperature, pH, and C/N ratio on the immobilization of Cd²⁺ by SRB in aqueous solution under an anoxic environment. The experimental results showed that under the conditions of initial concentration of Cd²⁺ within 0 mg/L~30 mg/L, initial concentration of SO₄²⁻ within 1200 mg/L, temperature within 25 °C~35 °C, pH neutral, and C/N ratio of 20:1, the immobilization rate of Cd²⁺ by SRB is above 90%. The characterization results showed that bioadsorption and chemical precipitation were the main mechanisms of SRB immobilization of Cd²⁺ in an anoxic environment.

Keywords: sulfate-reducing bacteria; Cd²⁺; anoxic environment; immobilized mechanism



Citation: Liao, L.; Li, Q.; Yang, Y.; Xu, R.; Zhang, Y. Immobilization Behavior and Mechanism of Cd²⁺ by Sulfate-Reducing Bacteria in Anoxic Environments. *Water* **2024**, *16*, 1086. <https://doi.org/10.3390/w16081086>

Academic Editor: Alejandro Gonzalez-Martinez

Received: 20 March 2024

Revised: 29 March 2024

Accepted: 29 March 2024

Published: 10 April 2024



Copyright: © 2024 by the authors. Licensee MDPI, Basel, Switzerland. This article is an open access article distributed under the terms and conditions of the Creative Commons Attribution (CC BY) license (<https://creativecommons.org/licenses/by/4.0/>).

1. Introduction

In recent years, with the rapid advancement of industrialization and urbanization processes, heavy metal pollution, especially heavy metal pollution in water bodies, has become a global environmental issue [1]. Among them, cadmium (Cd) is one of the heavy metals with the greatest environmental impact [2]. Cd in water bodies mainly comes from activities such as electroplating, paint pigments, batteries, fertilizers, and mining [3]. Cd can accumulate in organisms through biological accumulation. Excessive intake of Cd by humans can lead to various toxic effects on the bones, kidneys, liver, cardiovascular system, endocrine system, and reproductive system, as well as carcinogenicity and genetic diseases [4]. The World Health Organization specifies the allowable concentration of Cd in drinking water as 0.003 mg/L, while China sets it at 0.005 mg/L [5]. Additionally, China mandates a cadmium wastewater discharge standard of 0.1 mg/L. Therefore, it is necessary to treat wastewater containing Cd before discharge.

Currently, various treatment technologies such as chemical precipitation, coagulation/flocculation, ion exchange, electro dialysis, membrane filtration, adsorption, etc., have been developed for the remediation of heavy metal pollution in water bodies [6]. The microbial remediation of heavy metals is widely utilized by scientists due to its high cost-effectiveness, environmental friendliness, and simplicity of operation. Microorganisms have the capability to alter the form of heavy metals present in the environment by influencing their chemical or physical properties. This enables them to convert heavy metals into less toxic oxidation states or reduce their mobility, thereby achieving the immobilization or removal of heavy metals from water bodies or soil. Among the myriad of microorganisms involved in heavy metal removal, biogenic sulfide precipitation technology, combining mechanisms such as biosorption, bioaccumulation, and bioprecipitation, has emerged as

an effective solution for removing toxic heavy metals (including Cd) from wastewater [7]. Compared to traditional methods, this approach offers economic, efficient, and stable removal of heavy metals. Sulfate-reducing bacteria utilize sulfate as a terminal electron acceptor, metabolizing organic substrates under anaerobic conditions to convert sulfate to sulfide, which then forms stable precipitates when combined with heavy metals [8]. Li et al. [9] demonstrated that sulfate-reducing bacteria (SRB) achieve removal rates of common heavy metal ions (such as Cd, Cu, and Pb) in wastewater of over 94%. Dong et al. [10] found that by adding SRB to acid mine drainage (AMD) containing varying concentrations of Fe, Mn, and Cu, SRB maintained high removal rates of Fe within the concentration range of 0–300 mg/L. Over the past few decades, SRB processes have been widely applied in treating industrial wastewater containing high concentrations of heavy metals and sulfates generated from industries such as pulp and paper, textile, mining, and papermaking [11].

It is generally believed that sulfate-reducing bacteria (SRB) are strictly anaerobic organisms. However, recent studies have confirmed that sulfate reduction can occur in aerobic environments. For instance, some SRB oxidize polyglucose to produce ATP, thereby minimizing oxidative stress, which is considered a mechanism for SRB survival in aerobic environments. These SRB can quickly restore sulfate reduction activity upon transition from aerobic to anaerobic environments [12,13]. *Desulfuromonas*, isolated from microbial mats in saline environments, exhibits rapid growth rates when exposed to aerobic conditions, indicating its ability to grow using oxygen. However, there is limited research on the growth mechanism of SRB in anoxic environments and their mechanisms of bio-immobilization of Cd. This is mainly because the addition of oxygen makes the respiratory mechanism of SRB more complex compared to anaerobic environments [14]. The biological stabilization mechanism of SRB in aerobic environments is not fully understood, limiting their application in aerobic environments.

This study inoculated cultivated sulfate-reducing bacteria (SRB) into anoxic environments containing heavy metal Cd. By varying factors such as pH, temperature, initial SO_4^{2-} concentration, initial Cd^{2+} concentration, and C/N ratio, the study examined the effects of these factors on SRB growth under anoxic conditions, as well as the behavior and mechanisms of SRB in immobilizing Cd^{2+} .

2. Materials and Methods

2.1. Source and Cultivation Conditions of SRB

In this study, the sulfate-reducing bacterial strain (*Desulfovibrio desulfuricans* subsp. *Desulfuricans*) was provided by the Key Laboratory of Biometallurgy of the Ministry of Education at Central South University. After activation, the strain was enriched in anaerobic bottles using modified Baar's sulfate-reducing medium [15]. The composition of the medium is as follows: MgSO_4 (2 g/L), sodium citrate (5 g/L), $\text{CaSO}_4 \cdot 2\text{H}_2\text{O}$ (1 g/L), NH_4Cl (1 g/L), K_2HPO_4 (1 g/L), sodium lactate (3.5 g/L), and yeast extract (1 g/L). The pH was adjusted to 7.0–7.5, and the medium was sterilized at 121 °C for 30 min. After inoculating the strain, 2% (v/v) of autoclaved ferrous ammonium sulfate solution ($\text{Fe}(\text{NH}_4)_2(\text{SO}_4)_2$) (5%) was added. In the anaerobic glove box, 300 mL of the medium was transferred into a 500 mL anaerobic bottle. Subsequently, 10% (v/v) of the bacterial suspension was inoculated, and the bottom of the bottle was purged with N_2 before and after inoculation to remove air as much as possible. The anaerobic bottles were then placed in an oscillating incubator set at 30 °C and 160 r/min for 5 days. After cultivation, the bacterial suspension was used for subsequent Cd^{2+} immobilization experiments. The chemicals used in this study were all purchased from China National Pharmaceutical Group and were of analytical grade.

2.2. Biological Immobilization of Cd^{2+} by SRB under Anoxic Conditions

The immobilization experiments were conducted in 500 mL anaerobic bottles within an oscillating incubator. The experiment investigated the effects of initial Cd^{2+} concentration (10 mg/L to 40 mg/L), initial SO_4^{2-} concentration (800 mg/L to 2000 mg/L), temperature

(20 °C to 35 °C), initial pH (4.5 to 7.5), and C/N ratio (20:3 to 20:1) on the immobilization of Cd^{2+} by SRB under anoxic conditions [16].

Under room temperature conditions, a solution containing a certain concentration of Cd^{2+} was prepared using $\text{Cd}(\text{NO}_3)_2$, and a certain amount of Cd^{2+} solution was added to 300 mL of medium in the anaerobic bottle, which was then placed in the anoxic chamber. The bottle was purged with high-purity N_2 for 3 min, sealed with blue butyl rubber and aluminum caps to establish an anoxic environment [17]. After inoculating with 30 mL of cultured bacterial suspension, the bottles were transferred to the oscillating incubator (with a speed of 160 r/min). Subsequently, no additional nutrients were added to the medium. During the experiment, 20 mL of liquid samples were collected every 24 h, seven times in total. The collected samples were centrifuged at high speed (4000 r/min), and the supernatant was collected to measure the Eh, pH, bacterial concentration (OD600 value), SO_4^{2-} concentration, and Cd^{2+} concentration in the solution. Each experiment was performed in triplicate.

2.3. Characterization of Metallic Precipitates

The bacterial suspension collected after 7 days of cultivation was centrifuged in a high-speed centrifuge for 10 min at 8000 r/min to separate the solid and supernatant. The solid was washed repeatedly with deionized water and then placed in a vacuum freeze-dryer for 24 h to dry [10]. Then, the dried precipitation was tested by SEM–EDS and XPS.

2.4. Analytical Methods

The pH and Eh were measured using a pH meter (Leici PHS-3C). The concentration of SO_4^{2-} was determined using the barium chromate spectrophotometric method. The OD600 value was determined using a UV–visible spectrophotometer. The concentration of Cd^{2+} was determined using a flame atomic absorption spectrometer. Surface morphology and structure were observed using scanning electron microscopy (SEM, Helios NanoLab G3 UC or Quanta FEG 250, FEI, Lausanne, Switzerland) and energy-dispersive X-ray spectroscopy (EDS). The surface chemical composition and state of SRB before and after Cd^{2+} immobilization were analyzed using X-ray photoelectron spectroscopy (XPS, Escalab 250Xi, Thermo Fisher, Oxford, UK).

3. Results and Discussion

3.1. Analysis of Factors Influencing the Immobilization of Cd^{2+} by SRB

3.1.1. The Influence of Initial Cd^{2+} Concentration on the Immobilization Performance of SRB

The Cd^{2+} in the solution can disrupt microbial cell wall synthesis, respiratory chain function, and metal ion homeostasis, leading to oxidative stress, DNA damage, and energy metabolism disorders, ultimately causing extreme cytotoxic effects [18]. As shown in Figure 1a,b, with the increase in SRB cultivation time, the pH of the solution gradually increases from 6.5 to around 7.3, while the Eh value shows a decreasing trend. This is because during the sulfate reduction process, SRB oxidize organic carbon to produce HCO_3^- , causing the pH of the solution to increase [19]. In Figure 1c, the trend of OD600 changes indicates rapid growth of SRB within 24 h after inoculation, with a significant increase in bacterial concentration. However, bacterial growth slows down from day 2 to day 7. Moreover, the higher the initial Cd^{2+} concentration, the lower the final OD value (Figure 1c), which may be attributed to the inhibition of SRB growth under high Cd^{2+} concentration stress. Liu et al. [20] proposed that in environments with low concentrations of Cd^{2+} , the permeability of SRB cells slightly increases, making it easier for nutrients in the medium to be absorbed. However, when the Cd^{2+} concentration increases to a certain level, the cell membrane of SRB is severely damaged, limiting bacterial growth. As shown in Figure 1e, when the initial Cd^{2+} concentration is less than 30 mg/L, SRB show high removal efficiency for Cd, reaching over 94% within 7 days. However, when the initial Cd^{2+} concentration is 40 mg/L, the removal rate of Cd decreases to below 80%. The initial

concentration of heavy metal ions has a significant impact on microbial activity. Under high Cd^{2+} concentrations, bacterial enzymes are damaged and inactivated [21], reducing their reduction capacity, ultimately leading to lower removal rates of SO_4^{2-} (Figure 1d) and Cd^{2+} (Figure 1e).

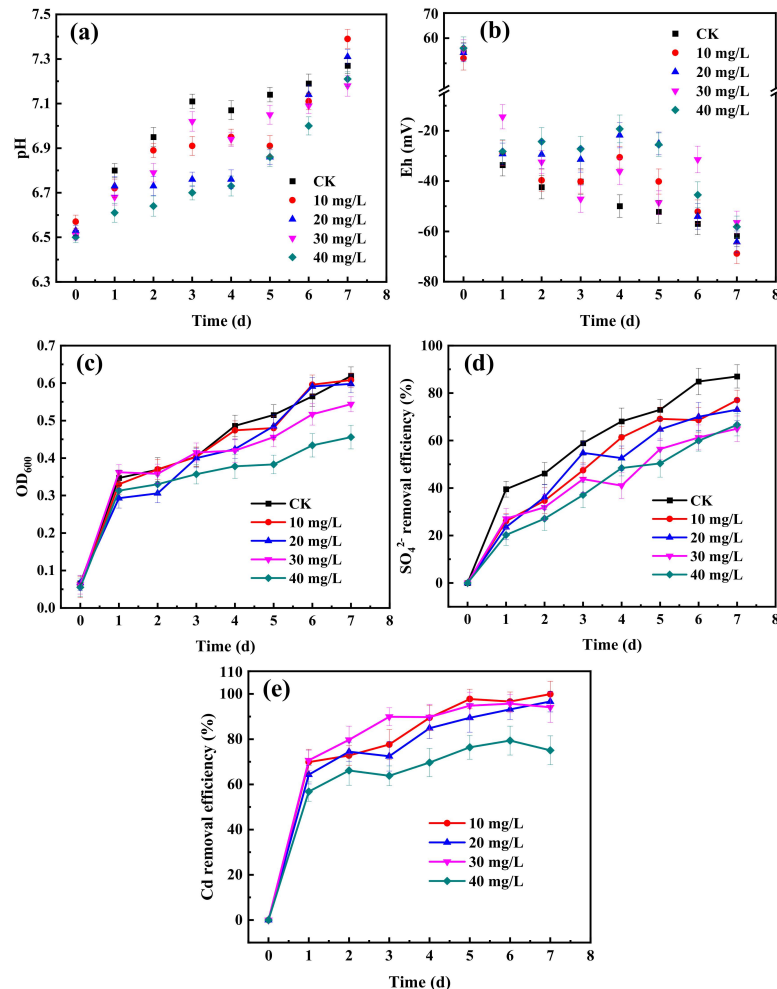


Figure 1. Effect of Cd^{2+} concentration on SRB growth and Cd^{2+} immobilization, (a) pH, (b) Eh, (c) OD_{600} , (d) SO_4^{2-} removal rate, (e) Cd^{2+} removal rate.

3.1.2. The Influence of Initial SO_4^{2-} Concentration on the Immobilization Performance of SRB

Under conditions with a pH of 6.5, the influence of SO_4^{2-} concentration on SRB-mediated Cd removal was investigated, and the results are depicted in Figure 2. Under different SO_4^{2-} concentration conditions, the pH during microbial growth exhibited an increasing trend (Figure 2a). The results indicate that within 3 days of inoculation with SRB, the pH of the solution increased from 6.5 to 7.0–7.4, while the pH remained relatively stable from day 3 to day 7. This could be attributed to the reduction in sodium lactate, which provides electrons for sulfate reduction, during the sulfate reduction process, leading to a decrease in HCO_3^- production and an increase in acetic acid content [22]. The OD_{600} measurement results showed that the highest OD_{600} value was observed when the initial SO_4^{2-} concentration was 1200 mg/L, reaching 0.82, indicating optimal SRB growth under this condition (Figure 2c). The removal efficiency of Cd^{2+} by SRB exhibited an increasing trend followed by a decrease with increasing initial SO_4^{2-} concentration (Figure 2e). Specifically, when the initial SO_4^{2-} concentration was 1200 mg/L, SRB exhibited the best removal efficiency for Cd^{2+} , with a removal rate of 99.42% after 7 days. However, when the initial SO_4^{2-} concentration was 800 mg/L, the removal rate was only 82.47%. This may be related

to the COD/SO₄²⁻ ratio, as previous studies have shown that the initial COD/SO₄²⁻ ratio is one of the key factors affecting SRB growth. When the initial COD/SO₄²⁻ ratio is 3, the production of ATP in SRB and the removal efficiency of heavy metals are both higher than those at other ratios [23,24]. Therefore, both excessively high and low SO₄²⁻ concentrations can lead to a decrease in SRB's ability to remove Cd. This experiment identified the optimal initial SO₄²⁻ concentration as 1200 mg/L.

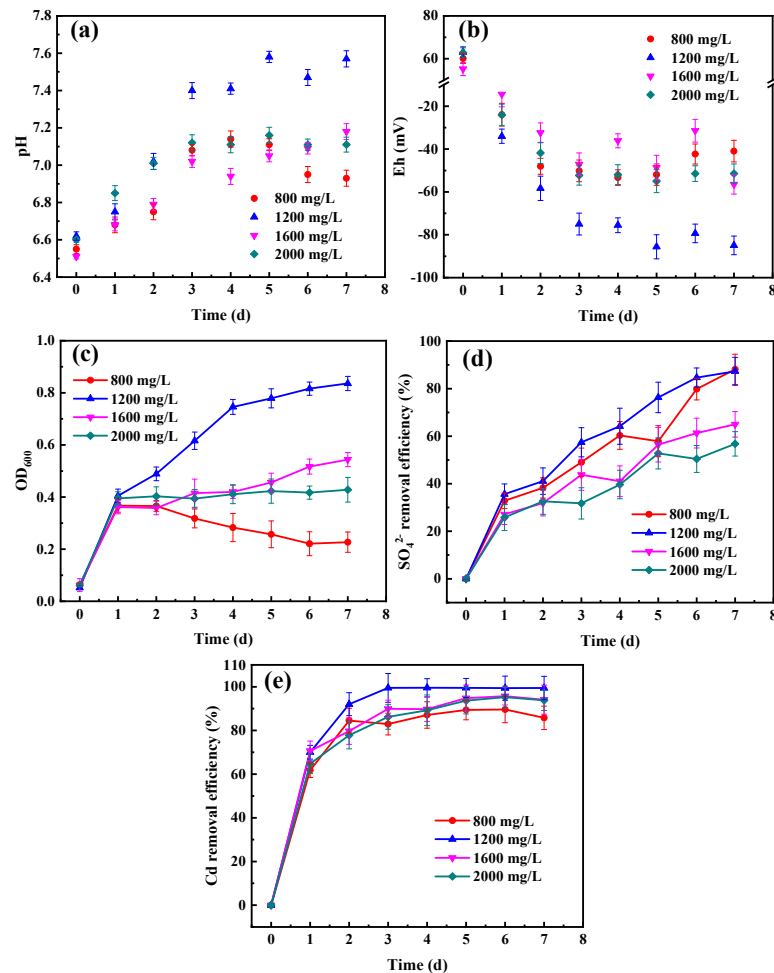


Figure 2. Effect of SO₄²⁻ concentration on SRB growth and Cd²⁺ immobilization, (a) pH, (b) Eh, (c) OD₆₀₀, (d) SO₄²⁻ removal rate, (e) Cd²⁺ removal rate.

3.1.3. The Influence of Temperature on the Immobilization Performance of SRB

Microbial cell growth involves a series of enzyme-catalyzed reactions, and excessively high or low temperatures can inhibit the activity of certain enzymes in these cells. This can have adverse effects on cell growth and product synthesis, leading to changes in morphology, metabolism, and microbial toxicity, and even cell death [25]. The growth status of SRB, as well as the removal rates of SO₄²⁻ and Cd²⁺ at different temperatures, are depicted in Figure 3. Under each temperature condition, the pH of the solution showed a gradual increase with the growth of the bacterial strains, with the most significant increase observed at 30 °C (Figure 3a). This is mainly because SRB exhibit high growth activity and a large population size at this temperature, resulting in higher metabolic alkalinity [26]. Figure 3c indicates that the OD₆₀₀ value of the solution was lowest at 20 °C and highest at 30 °C, further suggesting optimal SRB growth conditions at this temperature, which is consistent with the findings reported by Sokolova [27]. There were no significant differences in SRB activity and their removal rates of SO₄²⁻ (Figure 3d) and Cd²⁺ (Figure 3e) observed at temperatures between 25 °C and 35 °C. At 35 °C, the removal rates of SO₄²⁻ and Cd²⁺

were the highest, reaching 66.81% and 96.11%, respectively. However, at 20 °C, the removal rate of Cd^{2+} by SRB was less than 90%. This may be because low temperatures reduce the activity of SRB cell membrane proteins, limiting the transport capacity of the cell membrane for electron donors and acceptors, thereby affecting metabolism [16]. Therefore, this study identifies the optimal temperature range for SRB-mediated Cd^{2+} immobilization as 25 °C to 35 °C.

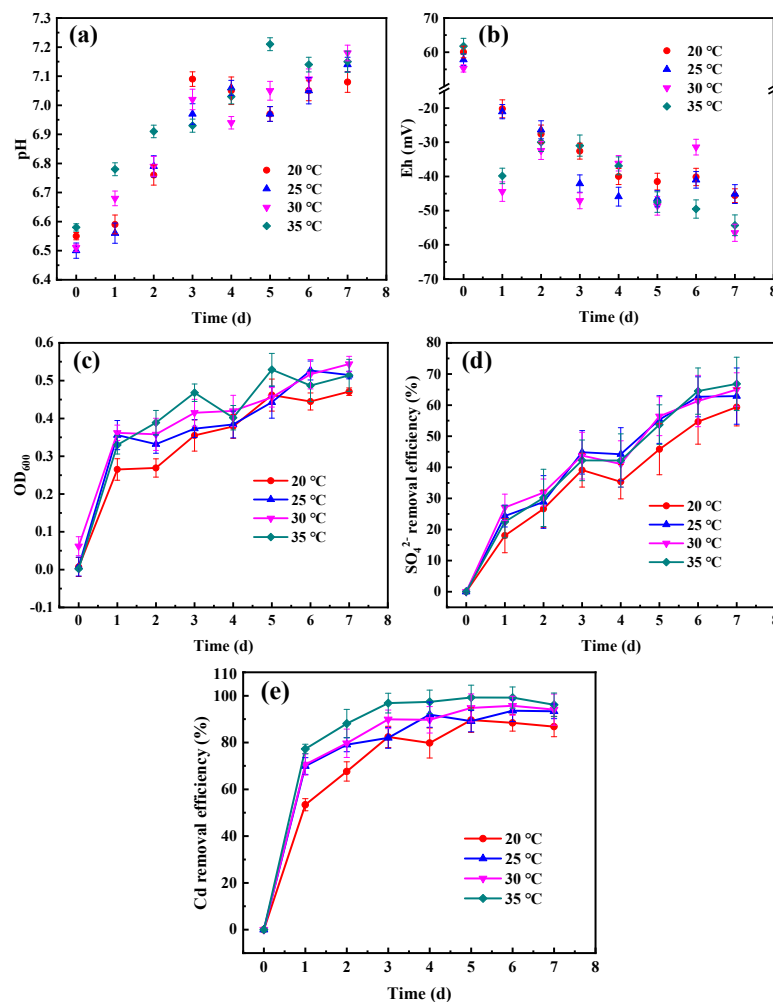


Figure 3. Effect of temperature on SRB growth and Cd^{2+} immobilization, (a) pH, (b) Eh, (c) OD₆₀₀, (d) SO_4^{2-} removal rate, (e) Cd^{2+} removal rate.

3.1.4. The Influence of Initial pH on the Immobilization Performance of SRB

Environmental pH is one of the major factors strongly influencing microbial metabolic activities and bacterial communities, and the transport of nutrients into and out of bacterial cells is usually determined by pH [28]. As indicated in Figure 4, SRB activity (Figure 4c) and its efficiency in removing Cd^{2+} (Figure 4e) exhibit high sensitivity to pH. Experimental results demonstrate that at neutral pH levels of 6.51 and 7.13, the pH (Figure 4a) and Eh (Figure 4b) of the solution remain relatively stable, and SRB exhibit high removal rates for both SO_4^{2-} (Figure 4d) and Cd^{2+} (Figure 4e). Under these two pH conditions, after 7 days of testing, the removal rates of SO_4^{2-} were 64.99% and 89.51%, respectively, while the removal rates of Cd^{2+} were 94.08% and 96.57%. At a pH of 4.62, significant differences were observed compared to neutral conditions. By the seventh day, the pH had risen to 6.21, the Eh had decreased from 100 mV to −10 mV, and the removal rates of SO_4^{2-} and Cd^{2+} were only 36.61% and 25.89%, respectively. Figure 4c indicates that the growth level of SRB at initial pH levels of 6.51 and 7.13 is significantly higher than at the two lower pH levels. On one hand, at lower pH levels, active sites are protonated, and SRB surfaces carry positive

charges, leading to competition between H^+ (or H_3O^+) and metal cations for binding sites. As the pH increases, SRB surfaces carry more negative charges, resulting in an increase in the bioadsorption of positively charged metal ions [29]. On the other hand, the metabolic byproducts of SRB have potential toxicity in acidic environments (such as hydrogen sulfide and organic acids), and at low pH levels, the high solubility of Cd^{2+} in the solution can lead to enzyme inactivation and protein denaturation within the bacteria [30,31]. These experimental results suggest that the optimal pH for SRB growth is between 6.5 and 7.1, and SRB are not suitable for the biological fixation of Cd^{2+} at lower pH levels [32].

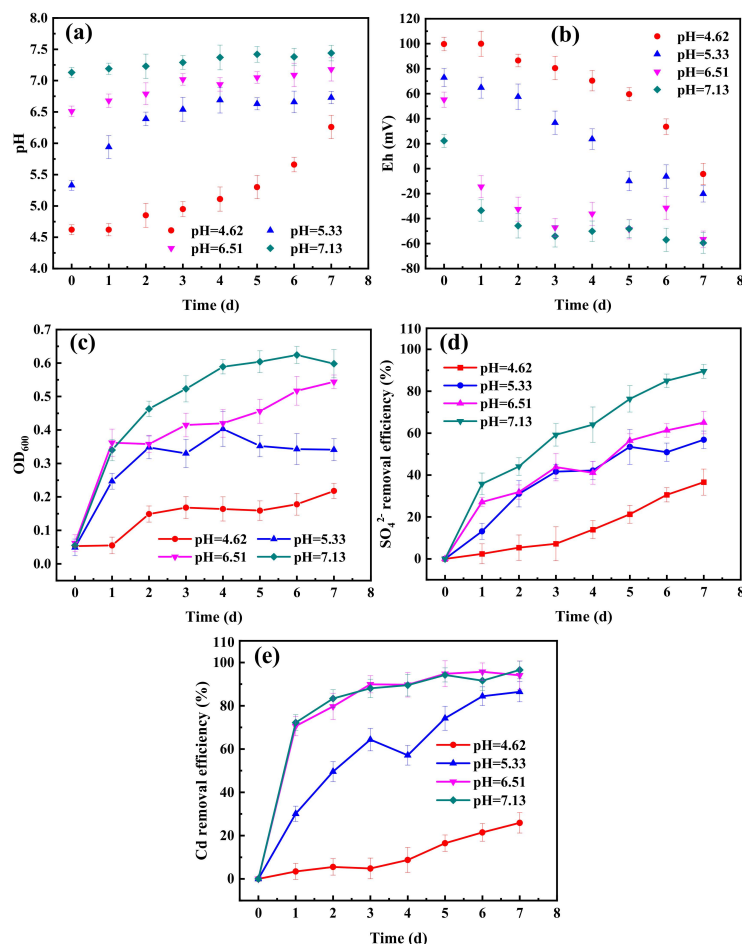


Figure 4. Effect of pH on SRB growth and Cd^{2+} immobilization, (a) pH, (b) Eh, (c) OD_{600} , (d) SO_4^{2-} removal rate, (e) Cd^{2+} removal rate.

3.1.5. The Influence of Carbon-to-Nitrogen (C/N) Ratio on the Immobilization Performance of SRB

Carbon (C) and nitrogen (N) are crucial nutrients for all organisms, and maintaining an appropriate balance in their metabolism is essential for optimal cell growth [33]. As shown in Figure 5a–c, under five different C/N ratio conditions, after 7 days of microbial remediation, the pH of the solution increased from weakly acidic to neutral (Figure 5a). At the same time, the Eh showed a decreasing trend (Figure 5b). OD_{600} measurements revealed that the most favorable C/N ratio for SRB growth was 40:3. Carbon (C) and nitrogen (N) are crucial nutrients for all organisms, and maintaining an appropriate balance in their metabolism is essential for optimal cell growth [33]. As shown in Figure 5a–c, under five different C/N ratio conditions, after 7 days of microbial remediation, the pH of the solution increased from weakly acidic to neutral (Figure 5a). At the same time, the Eh showed a decreasing trend (Figure 5b). OD_{600} measurements revealed that the most favorable C/N ratio for SRB growth was 40:3 (Figure 5c). Figure 5d,e demonstrate that

when the C/N ratio was 40:3, SRB exhibited the highest removal rates for SO_4^{2-} and Cd^{2+} , reaching 68.89% and 99.36%, respectively, on the seventh day. Conversely, when the C/N ratio was 20:1, the removal efficiencies of SRB for SO_4^{2-} and Cd^{2+} were the lowest, at 59.81% and 92.81%, respectively, on the seventh day. Moreover, excessively high (20:1) or low (20:3) C/N ratios both restricted SRB growth and affected the removal efficiencies of SO_4^{2-} and Cd^{2+} . Since C and N are the most abundant elements in cells, coordination mechanisms are required to avoid inefficient metabolism. Nitrogen assimilation depends on the availability of the carbon skeleton in biosynthesis. Therefore, a limitation or excess supply of one element strongly affects the metabolism of the other [34]. According to the “stoichiometric decomposition theory” and the “microbial nitrogen acquisition hypothesis,” microbial activity is maximized, and decomposition rates are highest when the input of C, N, and substrate matches microbial demand, corresponding to the stoichiometric ratio of C and N [35,36]. Therefore, adding organic matter with an appropriate C/N ratio to the growth medium of SRB can enhance their metabolic capacity in heavy metal environments and improve their efficiency in metal immobilization. Under the five different C/N ratio conditions in the experimental design, the fixation efficiency of SRB for Cd^{2+} was above 90%, indicating a certain tolerance of this SRB strain to changes in the C/N ratio in a cadmium-containing environment. This result may suggest that the strain of SRB can flexibly regulate metabolic pathways under different carbon-to-nitrogen ratios to adapt to the presence of cadmium ions in the environment.

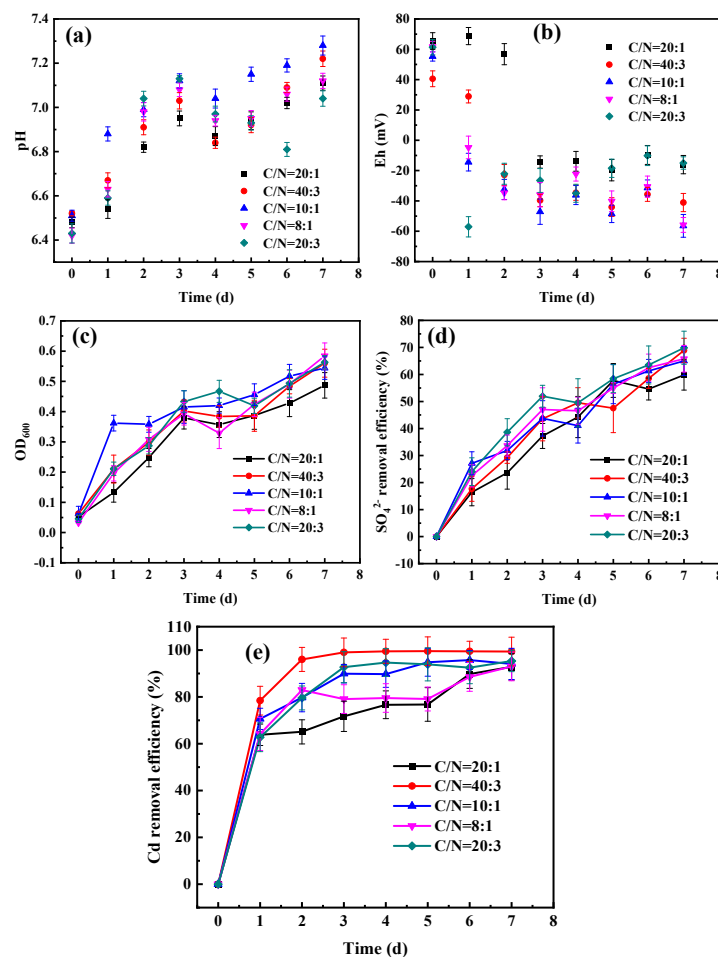


Figure 5. Effect of C/N ratio on SRB growth and Cd²⁺ immobilization, (a) pH, (b) Eh, (c) OD₆₀₀, (d) SO₄²⁻ removal rate, (e) Cd²⁺ removal rate.

3.2. SEM–EDS Analysis

Through SEM–EDS analysis, the morphological structure and chemical composition of SRB before and after Cd^{2+} fixation are shown in Figure 6. SEM images reveal that the surface of unreacted SRB (Figure 6a) is smooth with well-developed pore structures and abundant active adsorption sites, facilitating the adsorption of Cd^{2+} into the interior of SRB. After the reaction, the surface of SRB (Figure 6b) becomes rough with numerous folds, and elliptical insoluble substances can be clearly observed blocking surface pores, indicating the adsorption of substances onto the SRB surface. The EDS spectra clearly demonstrate that the main elements in SRB are C, N, and O, with elemental contents of 57.65%, 15.61%, and 23.28%, respectively. Additionally, there are trace amounts of P and S. In the EDS spectrum after the reaction (Figure 6b'), the presence of Cd is detected (with a content of 1.91%), confirming that the substance adsorbed on the surface of SRB is a Cd-containing precipitate. Based on these results, it is inferred that a precipitation reaction occurs during the process of SRB fixing Cd^{2+} , as shown in Equations (1) and (2):

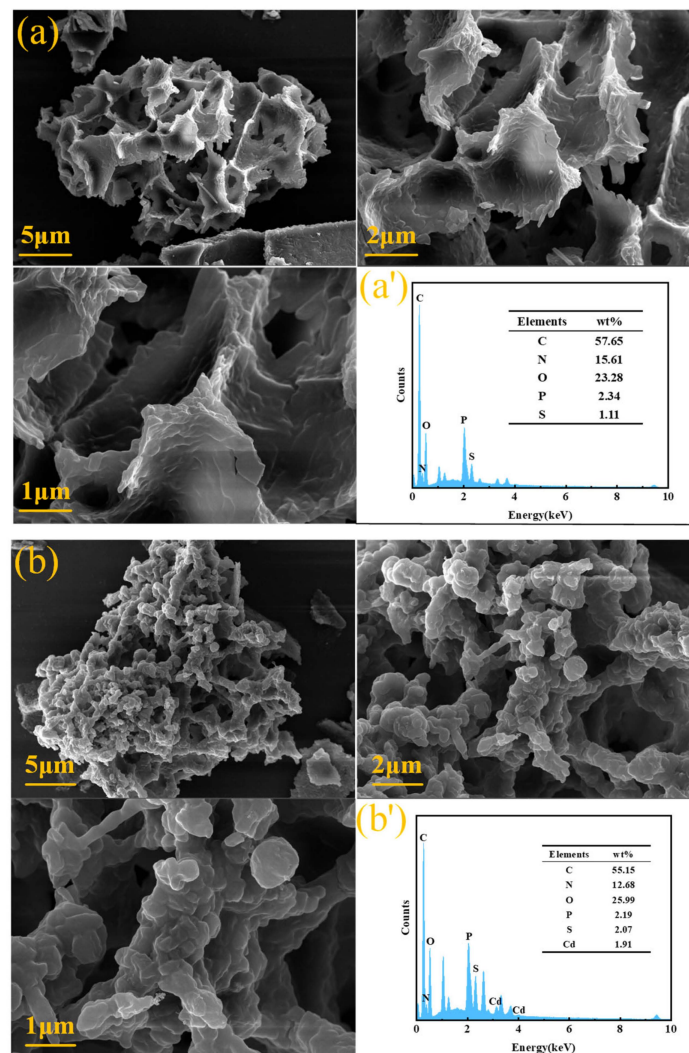


Figure 6. SEM images and EDS spectra before and after Cd^{2+} immobilization by SRB, (a)/(a') original SRB bacteria, (b)/(b') products after immobilization.

These equations illustrate the process of Cd^{2+} being adsorbed onto SRB surfaces and forming CdS and $\text{Cd}(\text{OH})_2$ precipitates.

3.3. XPS Analysis

Further investigation using XPS explored the surface chemical composition and binding forms of precipitates before and after SRB fixation of Cd. As shown in Figure 7a, atomic orbitals identifiable both before and after SRB fixation of Cd include C 1s, O 1s, N 1s, P 2p, and S 2p. In the scan spectrum after SRB fixation of Cd, characteristic peaks of Cd 3d can be clearly identified, and the binding energy of these peaks is around 405 eV, close to the characteristic peak of N 1s. Combining Figure 7b,c, it can be observed that the peak nearly overlapping with the N 1s characteristic peak is Cd 3d_{5/2}, indicating the immobilization of Cd^{2+} by SRB.

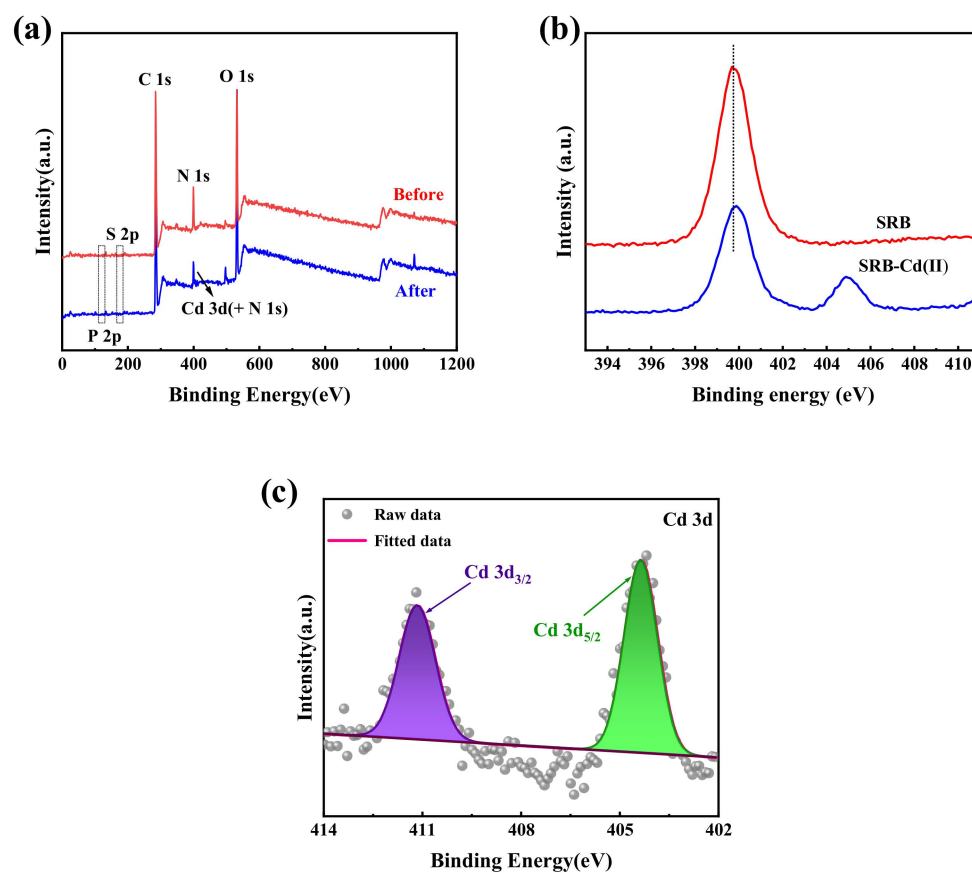


Figure 7. XPS analysis before and after Cd^{2+} immobilization by SRB, (a) full spectrum, (b) N 1s orbital spectrum, (c) Cd 3d orbital spectrum.

Figure 8 depicts the XPS spectra of C 1s, O 1s, P 2p, and S 2p orbitals before and after SRB fixation of Cd. Before and after immobilization, the C 1s orbitals exhibit three peaks, with the binding energies of C–O and C–C increasing from 286.18 eV to 286.38 eV and from 284.68 eV to 284.78 eV, respectively, while that of C=O decreases from 287.98 eV to 287.78 eV. This indicates the involvement of carbon groups in the SRB fixation process of Cd. Observation of the O 1s XPS spectra reveals an increase in the binding energies of all three peaks after immobilization compared to before, indicating that oxygen atoms can act as electron donors during Cd immobilization processes [37]. The P 2p spectrum can be divided into two components at 132.68 eV and 133.38 eV, attributed to P–C and O=P(OR)₃, respectively [38]. The changes in the peak areas of these two functional groups before and after the reaction suggest their involvement in Cd^{2+} fixation. The S 2p orbital spectrum before SRB immobilization of Cd consists of four peaks attributed to SO_4^{2-} (168.08 eV),

S_n^{2-} (163.88 eV), S_2^{2-} (163.08 eV), and S^{2-} (162.28 eV). After the reaction, the content of SO_4^{2-} and S_2^{2-} decreases significantly, while that of S_n^{2-} and S^{2-} increases, further confirming the fixation of Cd^{2+} by SRB and the formation of S-containing precipitates.

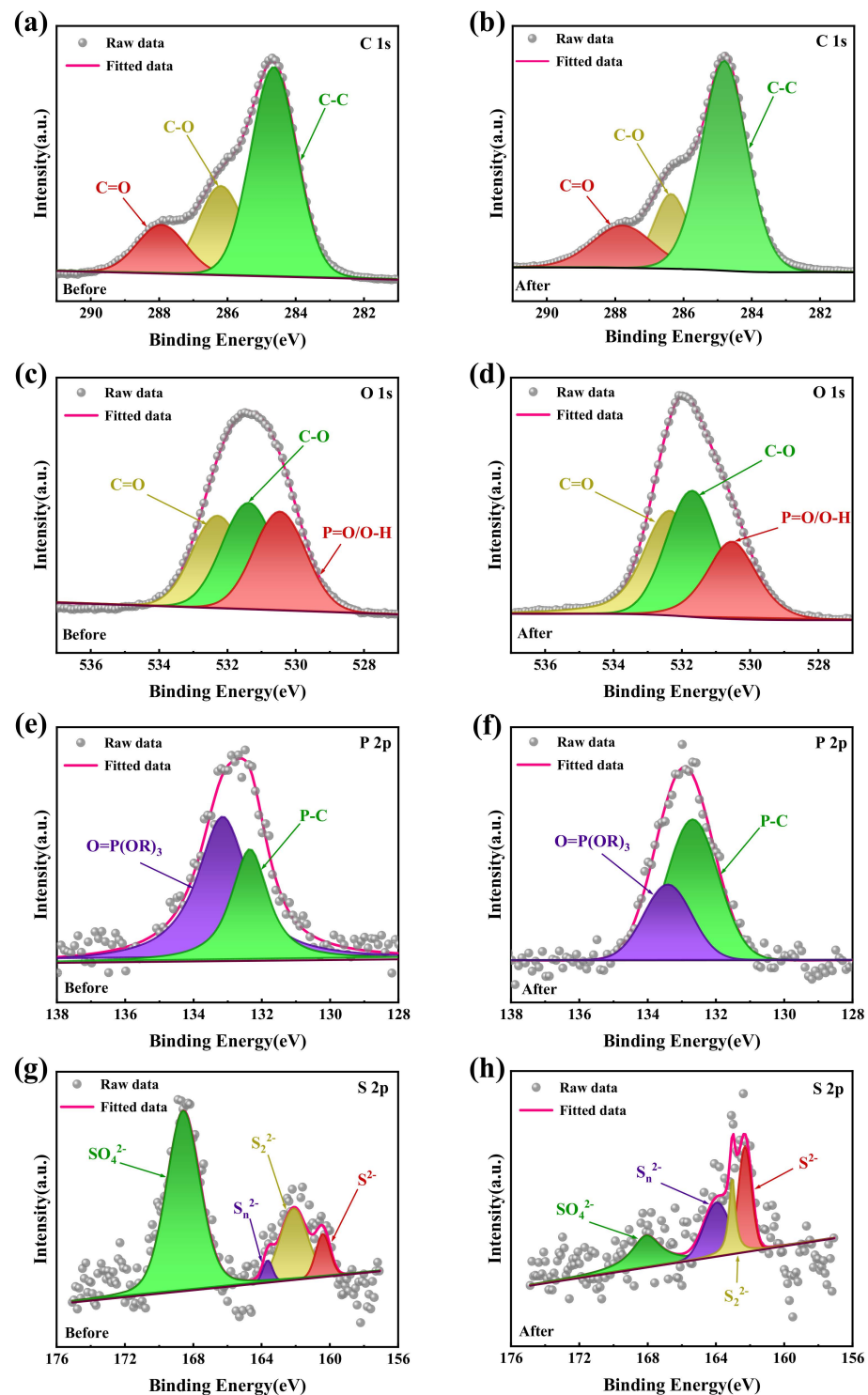


Figure 8. XPS analysis before and after Cd^{2+} immobilization by SRB, (a,c,e,g): C1s, O 1s, P2p, S2p orbital spectra before Cd^{2+} immobilization; (b,d,f,h): C1s, O 1s, P2p, and S2p orbital spectra after Cd^{2+} immobilization.

4. Conclusions

Given the potential hazards of Cd to the natural environment and human health, as well as the unclear understanding of the survival status of sulfate-reducing bacteria (SRB) and its Cd removal mechanism under anoxic conditions, we conducted a systematic study on the immobilization of Cd by SRB in wastewater. The optimal conditions for SRB-mediated Cd²⁺ immobilization in anoxic environments were obtained through conditional experiments in this study. By characterizing the metal precipitates, the immobilization mechanism was elucidated. The main conclusions obtained are as follows:

- (1) Under anoxic conditions, SRB demonstrates excellent immobilization efficiency for Cd²⁺ after enrichment cultivation in modified Baar's sulfate medium. When the initial Cd²⁺ concentration does not exceed 30 mg/L, the initial SO₄²⁻ concentration is 1200 mg/L, the temperature ranges from 25 °C to 35 °C, the pH is neutral, and the C/N ratio is 20:1, the fixation rate of Cd²⁺ by SRB exceeds 90%, and the SRB strains exhibit robust growth.
- (2) SEM-EDS and XPS analyses reveal that functional groups containing C, O, P, and S on SRB are involved in the immobilization process under anoxic conditions. Additionally, a precipitation reaction occurs during the immobilization of Cd²⁺ by SRB, resulting in the formation of CdS and Cd(OH)₂. Therefore, the primary mechanism of SRB immobilization of Cd²⁺ under anoxic conditions involves both biological adsorption and chemical precipitation.

Author Contributions: Conceptualization, L.L. and Q.L.; methodology, Q.L.; software, R.X. and Y.Z.; validation, L.L. and Q.L.; formal analysis, L.L. and R.X.; investigation, Y.Y.; data curation, L.L.; writing—original draft preparation, L.L. and Q.L.; writing—review and editing, R.X.; visualization, Y.Y. All authors have read and agreed to the published version of the manuscript.

Funding: This research was funded by the Key Research and Development Projects of the Science and Technology Department of Hunan Province, grant number 2022NK2057.

Data Availability Statement: The original contributions presented in the study are included in the article; further inquiries can be directed to the corresponding author.

Conflicts of Interest: The authors declare no conflicts of interest.

References

1. Zhao, Q.; Li, X.; Wang, Y.; Cheng, Y.; Fan, W. Long-term bioremediation of cadmium contaminated sediment using sulfate reducing bacteria: Perspective on different depths of the sediment profile. *Chem. Eng. J.* **2023**, *451*, 138697. [[CrossRef](#)]
2. Yuan, S.; Hong, M.; Li, H.; Ye, Z.; Gong, H.; Zhang, J.; Huang, Q.; Tan, Z. Contributions and mechanisms of components in modified biochar to adsorb cadmium in aqueous solution—ScienceDirect. *Sci. Total Environ.* **2020**, *733*, 139320. [[CrossRef](#)]
3. Zhu, X.; Song, T.; Lv, Z.; Ji, G. High-efficiency and low-cost α-Fe₂O₃ nanoparticles-coated volcanic rock for Cd(II) removal from wastewater. *Process Saf. Environ. Prot.* **2016**, *104*, 373–381. [[CrossRef](#)]
4. Uki-Osi, D.; Barali, K.; Javorac, D.; Orevi, A.B.; Bulat, Z. An overview of molecular mechanisms in cadmium toxicity. *Curr. Opin. Toxicol.* **2019**, *19*, 56–62.
5. Wang, X.; Hu, K.; Xu, Q.; Lu, L.; Wang, G. Immobilization of Cd Using Mixed Enterobacter and Comamonas Bacterial Reagents in Pot Experiments with *Brassica rapa* L. *Environ. Sci. Technol.* **2020**, *54*, 15731–15741. [[CrossRef](#)]
6. Tyagi, S.; Malik, W.; Annachhatre, A.P. Heavy metal precipitation from sulfide produced from anaerobic sulfidogenic reactor. *Mater. Today Proc.* **2020**, *32*, 936–942. [[CrossRef](#)]
7. Zhang, H.; Li, H.; Li, M.; Luo, D.; Chen, Y.; Chen, D.; Luo, H.; Chen, Z.; Li, K. Immobilizing Metal-Resistant Sulfate-Reducing Bacteria for Cadmium Removal from Aqueous Solutions. *Pol. J. Environ. Stud.* **2018**, *27*, 2851–2859. [[CrossRef](#)] [[PubMed](#)]
8. Bai, H.; Kang, Y.; Quan, H.; Han, Y.; Sun, J.; Feng, Y. Bioremediation of copper-containing wastewater by sulfate reducing bacteria coupled with iron. *J. Environ. Manag.* **2013**, *129*, 350–356. [[CrossRef](#)] [[PubMed](#)]
9. Li, X.; Lan, S.-M.; Zhu, Z.-P.; Zhang, C.; Zeng, G.-M.; Livu, Y.-G.; Cao, W.-C.; Song, B.; Yang, H.; Wang, S.-F.; et al. The bioenergetics mechanisms and applications of sulfate-reducing bacteria in remediation of pollutants in drainage: A review. *Ecotoxicol. Environ. Saf.* **2018**, *158*, 162–170. [[CrossRef](#)]
10. Dong, Y.R.; Gao, Z.Q.; Di, J.Z.; Wang, D.; Yang, Z.H.; Wang, Y.F.; Xie, Z.F. Study on the Effectiveness of Sulfate Reducing Bacteria to Remove Heavy Metals (Fe, Mn, Cu, Cr) in Acid Mine Drainage. *Sustainability* **2023**, *15*, 5486. [[CrossRef](#)]

11. Liamleam, W.; Annachhatre, A.P. Treating industrial discharges by thermophilic sulfate reduction process with molasses as electron donor. *Environ. Technol.* **2007**, *28*, 639–647. [[CrossRef](#)] [[PubMed](#)]
12. Mogensen, G.L.; Kjeldsen, K.U.; Ingvorsen, K. *Desulfovibrio aerotolerans* sp nov., an oxygen tolerant sulphatereducing bacterium isolated from activated sludge. *Anaerobe* **2005**, *11*, 339–349. [[CrossRef](#)] [[PubMed](#)]
13. Kjeldsen, K.U.; Joulain, C.; Ingvorsen, K. Oxygen Tolerance of Sulfate-Reducing Bacteria in Activated Sludge. *Environ. Sci. Technol.* **2004**, *38*, 2038–2043. [[CrossRef](#)] [[PubMed](#)]
14. Baumgartner, L.K.; Reid, R.P.; Dupraz, C.; Decho, A.W.; Buckley, D.H.; Spear, J.R.; Przekop, K.M.; Visscher, P.T. Sulfate reducing bacteria in microbial mats: Changing paradigms, new discoveries. *Sediment. Geol.* **2015**, *185*, 131–145. [[CrossRef](#)]
15. Antony, P.J.; Raman, R.K.S.; Kumar, P.; Raman, R. Corrosion of 2205 duplex stainless steel weldment in chloride medium containing sulfate-reducing bacteria. *Metall. Mater. Trans. a-Phys. Metall. Mater. Sci.* **2008**, *39A*, 2689–2697. [[CrossRef](#)]
16. Zhang, Z.; Zhang, C.; Yang, Y.; Zhang, Z.; Tang, Y.; Su, P.; Lin, Z. A review of sulfate-reducing bacteria: Metabolism, influencing factors and application in wastewater treatment. *J. Clean. Prod.* **2022**, *376*, 134109. [[CrossRef](#)]
17. Laso-Pérez, R.; Krukenberg, V.; Musat, F.; Wegener, G. Establishing anaerobic hydrocarbon-degrading enrichment cultures of microorganisms under strictly anoxic conditions. *Nat. Protoc.* **2018**, *13*, 1310–1330. [[CrossRef](#)] [[PubMed](#)]
18. Zhai, Q.X.; Xiao, Y.; Zhao, J.X.; Tian, F.W.; Zhang, H.; Narbad, A.; Chen, W. Identification of key proteins and pathways in cadmium tolerance of *Lactobacillus plantarum* strains by proteomic analysis. *Sci. Rep.* **2017**, *7*, 1182. [[CrossRef](#)] [[PubMed](#)]
19. Xu, Y.-N.; Chen, Y. Advances in heavy metal removal by sulfate-reducing bacteria. *Water Sci. Technol. A J. Int. Assoc. Water Pollut. Res.* **2020**, *81*, 1797–1827. [[CrossRef](#)]
20. Liu, Z.; Yang, S.; Bai, Y.; Xiu, J.; Yan, H.; Huang, J.; Wang, L.; Zhang, H.; Liu, Y. The alteration of cell membrane of sulfate reducing bacteria in the presence of Mn(II) and Cd(II). *Miner. Eng.* **2011**, *24*, 839–844. [[CrossRef](#)]
21. Guo, J.; Kang, Y.; Feng, Y. Bioassessment of heavy metal toxicity and enhancement of heavy metal removal by sulfate-reducing bacteria in the presence of zero valent iron. *J. Environ. Manag.* **2017**, *203*, 278–285. [[CrossRef](#)] [[PubMed](#)]
22. Oyekola, O.O.; van Hille, R.P.; Harrison, S.T.L. Study of anaerobic lactate metabolism under biosulfidogenic conditions. *Water Res.* **2009**, *43*, 3345–3354. [[CrossRef](#)] [[PubMed](#)]
23. Li, Y.-L.; Wang, J.; Yue, Z.-B.; Tao, W.; Yang, H.-B.; Zhou, Y.-F.; Chen, T.-H. Simultaneous chemical oxygen demand removal, methane production and heavy metal precipitation in the biological treatment of landfill leachate using acid mine drainage as sulfate resource. *J. Biosci. Bioeng.* **2017**, *124*, 71–75. [[CrossRef](#)] [[PubMed](#)]
24. Liamleam, W.; Annachhatre, A.P. Electron donors for biological sulfate reduction. *Biotechnol. Adv.* **2007**, *25*, 452–463. [[CrossRef](#)] [[PubMed](#)]
25. Huang, J.F.; Ou, Y.X.; Zhang, D.F.; Zhang, G.G.; Pan, Y.T. Optimization of the culture condition of *Bacillus mucilaginosus* using *Agaricus bisporus* industrial wastewater by Plackett-Burman combined with Box-Behnken response surface method. *AMB Express* **2018**, *8*, 141. [[CrossRef](#)] [[PubMed](#)]
26. Dong, Y.; Wang, J.; Gao, Z.; Di, J.; Wang, D.; Guo, X.; Hu, Z.; Gao, X.; Wang, Y. Study on Growth Influencing Factors and Desulfurization Performance of Sulfate Reducing Bacteria Based on the Response Surface Methodology. *ACS Omega* **2023**, *8*, 4046–4059. [[CrossRef](#)]
27. Sokolova, E.A. Influence of temperature on development of sulfate-reducing bacteria in the laboratory and field in winter. *Contemp. Probl. Ecol.* **2010**, *3*, 631–634. [[CrossRef](#)]
28. Tran, T.T.T.; Kannoorpatti, K.; Padovan, A.; Thennadil, S. Sulphate-Reducing Bacteria's Response to Extreme pH Environments and the Effect of Their Activities on Microbial Corrosion. *Appl. Sci.* **2021**, *11*, 2201. [[CrossRef](#)]
29. Quan, H.E.; Bai, H.; Han, Y.; Kang, Y.; Sun, J. Removal of Cu(II) and Fe(III) from aqueous solutions by dead sulfate reducing bacteria. *Front. Chem. Sci. Eng.* **2013**, *7*, 177–184. [[CrossRef](#)]
30. Rodrigues, C.; Nunez-Gomez, D.; Silveira, D.D.; Lapolli, F.R.; Lobo-Recio, M.A. Chitin as a substrate for the biostimulation of sulfate-reducing bacteria in the treatment of mine-impacted water (MIW). *J. Hazard. Mater.* **2019**, *375*, 330–338. [[CrossRef](#)]
31. Olaniran, A.O.; Balgobind, A.; Pillay, B. Bioavailability of Heavy Metals in Soil: Impact on Microbial Biodegradation of Organic Compounds and Possible Improvement Strategies. *Int. J. Mol. Sci.* **2013**, *14*, 10197–10228. [[CrossRef](#)] [[PubMed](#)]
32. Zhang, M.; Wang, H. Preparation of immobilized sulfate reducing bacteria (SRB) granules for effective bioremediation of acid mine drainage and bacterial community analysis. *Miner. Eng.* **2016**, *92*, 63–71. [[CrossRef](#)]
33. Zhou, W.; Colpa, D.I.; Geurkink, B.; Euverink, G.J.W.; Krooneman, J. The impact of carbon to nitrogen ratios and pH on the microbial prevalence and polyhydroxybutyrate production levels using a mixed microbial starter culture. *Sci. Total Environ.* **2022**, *811*, 152341. [[CrossRef](#)]
34. Zhang, C.C.; Zhou, C.Z.; Burnap, R.L.; Peng, L. Carbon/Nitrogen Metabolic Balance: Lessons from Cyanobacteria. *Trends Plant Sci.* **2018**, *23*, 1116–1130. [[CrossRef](#)]
35. Chen, R.R.; Senbayram, M.; Blagodatsky, S.; Myachina, O.; Dittert, K.; Lin, X.G.; Blagodatskaya, E.; Kuzyakov, Y. Soil C and N availability determine the priming effect: Microbial N mining and stoichiometric decomposition theories. *Glob. Chang. Biol.* **2014**, *20*, 2356–2367. [[CrossRef](#)]
36. Moorhead, D.L.; Sinsabaugh, R.L. A theoretical model of litter decay and microbial interaction. *Ecol. Monogr.* **2006**, *76*, 151–174. [[CrossRef](#)]

37. Zhao, R.; Li, X.; Sun, B.; Shen, M.; Tan, X.; Ding, Y.; Jiang, Z.; Wang, C. Preparation of phosphorylated polyacrylonitrile-based nanofiber mat and its application for heavy metal ion removal. *Chem. Eng. J.* **2015**, *268*, 290–299. [[CrossRef](#)]
38. Li, Y.; Xia, L.; Huang, R.; Xia, C.; Song, S. Algal biomass from the stable growth phase as a potential biosorbent for Pb(II) removal from water. *RSC Adv.* **2017**, *7*, 34600–34608. [[CrossRef](#)]

Disclaimer/Publisher’s Note: The statements, opinions and data contained in all publications are solely those of the individual author(s) and contributor(s) and not of MDPI and/or the editor(s). MDPI and/or the editor(s) disclaim responsibility for any injury to people or property resulting from any ideas, methods, instructions or products referred to in the content.